

ELECTRONICS LABORATORY • SYRACUSE, N.Y.



SOLID STATE IMAGE SENSOR RESEARCH PHASE I REPORT

Prepared by

G. C. Gerhard
R. E. Glusick
S. Razi
R. D. Stewart

Contract NAS-12-131

Prepared for

ELECTRONICS RESEARCH CENTER
NATIONAL AERONAUTICS AND SPACE ADMINISTRATION
CAMBRIDGE, MASSACHUSETTS

Electronics Laboratory
Syracuse, New York
and
Missile and Space Division
Philadelphia, Pennsylvania

GENERAL  ELECTRIC

N 67-19031	(ACCESSION NUMBER)	1	(THRU)
CR-82478	(PAGES)	[REDACTED]	(CATEGORY)
10	(NASA CR OR TMX OR AD NUMBER)		

FACILITY FORM 608

**SOLID STATE IMAGE SENSOR RESEARCH
PHASE I REPORT**

Prepared by

G. C. Gerhard
R. E. Glusick
S. Razi
R. D. Stewart

Contract NAS-12-131

Prepared for

**ELECTRONICS RESEARCH CENTER
NATIONAL AERONAUTICS AND SPACE ADMINISTRATION
CAMBRIDGE, MASSACHUSETTS**

Electronics Laboratory
General Electric Company
Syracuse, New York

Missile and Space Division
General Electric Company
Philadelphia, Pennsylvania

TABLE OF CONTENTS

<u>Section</u>	<u>Page</u>
INTRODUCTION.	iii
I. GENERAL CONSIDERATIONS.	1
II. SPECIFIC WAVELENGTH BANDS.	5
A. THE 10 - 12 MICRON REGION	5
B. THE 2.5 - 5.0 MICRON REGION.	14
C. THE VISIBLE REGION.	18
III. ELECTRONIC CIRCUIT TECHNIQUES.	23
IV. CONCLUSIONS AND RECOMMENDATIONS.	33
V. REFERENCES.	36

LIST OF ILLUSTRATIONS

<u>Figure No.</u>	<u>Title</u>	<u>Page</u>
1.	Liquidus - Solidus Curves for HgTe - CdTe.	8
2.	Energy Band Gap Relationship for HgCdTe and PbSnTe.	9
3.	Signal Amplifier and Conditioner	24
4.	Sampling Mode of Operation	24
5.	Single Detector Response to Optical Input	27
6.	Charge Storage - High Impedance Detectors	28
7.	Flux Linkage Storage - Low Impedance Detectors.	28
8.	Low Impedance Detectors and Charge Storage	28
9.	Linear Array Diode Switching.	29
10.	Matrix Array - Diode Switching.	29
11.	Matched Pair Detectors for Balancing Out Dark Current	30
12.	Synchronous Light Chopper and Mode Switch for Balancing Out Dark Current	30
13.	Current-Mode Emitter Coupled Drivers High Impedance Devices	32
14.	Low Impedance Circuit Using B-C Capacity of Transistor for Storage.	32
15.	Comparison of the Three Wavelengths of Interest	34

INTRODUCTION

This report concludes the first phase of the program "Solid State Image Sensor Research." During this phase, the capabilities and limitations of image sensing systems in the 0.4 to 15 micron wavelength band were determined and studied. During the course of this study, it was established that the bands of greatest interest were the visible, the 2.5 - 5 micron band, and the 10 - 12 micron band.

The studies undertaken included both the detectors and the readout capabilities required to adequately and optimally use the detectors in array operation. Cooling of the arrays and the scanning electronics is a necessary part of the IR systems and was included in the evaluation.

This report first details the detector materials, fabrication techniques and electronic scanning requirements; then, a set of conclusions and recommendations are given for future development and anticipated results in the three spectral bands of interest.

I. GENERAL CONSIDERATIONS

A. DETECTORS

The following general considerations are relevant to IR detectors regardless of wavelength:

- a) Thin film versus single crystal
- b) Extrinsic versus intrinsic detection
- c) Mode of operation: photoconductive, photovoltaic, photoelectromagnetic, photoemissive, Dember effect
- d) Operating temperature
- e) Response time
- f) Impedance
- g) Detectivity D^*
- h) Size and construction, including housing, windows, etc. for cooled detectors.

Each one of the above characteristics are briefly discussed below.

a) Thin film versus single crystal: In general thin film detectors are more non-uniform and less reproducible than single crystal detectors. Because of the thin layer, thin film detectors are more susceptible to damage by ultraviolet radiation, high ambient temperature, etc. For most single crystal detectors, semiconductor technology can generally be used to fabricate detectors and arrays.

b) Extrinsic detectors are less desirable because of 1) the need for critical doping control, 2) lower responsivity, and 3) lower optical absorption coefficient. The last feature requires large length of the material in the direction of the incident radiation which may be impractical in detector and array fabrication.

c) The most common modes of operation are photoconductive and photovoltaic. Photovoltaic operation requires that material be synthesized with both p- and n-type dopings, while for photoconductors it is important to have a low dark current which means the material should either have low intrinsic carrier concentration or be somehow compensated. Photovoltaic detectors may offer inherent electrical isolation and charge storage capability which is desirable for array fabrication and readout, while the high impedance of photoconductive detectors is also desirable for electronic readout. For photon noise limited operation, photovoltaic detection gives theoretically higher signal/noise ratio (by a factor of $\sqrt{2}$), although detectors actually fabricated from the same material but operating in the two different modes do not seem to confirm the theory. Photovoltaic detectors in general have lower response time than photoconductive detectors.

d) Obviously, the higher the permissible operating temperature of a detector, the more desirable it is. However, many detectors, particularly the extrinsic ones, have to be cooled to minimize thermal ionization of the impurities. In addition, low band gap intrinsic detectors (which are required for longer wavelength infrared detection) also need cooling in order to minimize the competing thermal (bolometric) effects.

c) Response time consideration is dependent on the particular detector and array requirements (for example, density, frame time, etc), requiring a low response time for high density arrays. However, for extrinsic detectors the responsivity of a detector is a direct function of the product ($\mu\tau$) where τ is the lifetime of the impurity state involved. In a case where τ is the determining factor in response time, one would have to compromise between high responsivity and low response time.

f) Detector impedance is important both from noise and readout stand-points. If the impedance is extremely high, the associated thermal noise would be correspondingly high and there would be problems of electrical pickup and microphonic noise. On the other hand, too low an impedance creates difficulties in charge storage type of readout. It appears that impedance in the range of 1 k Ω to 1 megohm is ideal. Equally important in the case of photoconductor, is the ratio of light to dark impedance which should be as high as possible.

g) Detectivity: Obviously the higher the detectivity in the desired wavelength region the better. An ideal photo response is one which has maximum detectivity in the range of the source spectrum and zero beyond. Detectivity is a function of various parameters, for example, field of view, chopping frequency, noise bandwidth, wavelength; all of which must be specified for a fair comparison of various detectors.

h) Detector size varies from 0.001" to 0.1" on edge, depending on specific needs. Various types of housings and windows are available for cooled detectors. Where a window is used, the transmission of the window must be taken into account in detector performance calculation. Details of housings and windows can be found in any standard infrared text book.

B. SPECTRAL COVERAGE FOR ADVANCED METEOROLOGICAL SATELLITES

There are many potential users of weather satellite information. Each potential user has data requirements for operations and research with varying spatial and temporal scales for each phenomenon. Surveys have been made through literature search and interviews with scientists which cover a broad range of applications.

The most significant output of satellite-borne infrared sensors for meteorological purposes is information on the temperature of various levels of the earth's atmosphere and that of the earth's surface. The spectral regions of high atmospheric transmission are best for measurement of surface temperature and the regions of high absorption are ideal for measurement of effective temperature at high altitudes at the top of the attenuating portion of the atmosphere.

Earth surface and troposphere can be investigated from satellites only by means of radiation analysis. Sources might eventually include not only long wavelength self-emission of earth and atmosphere and reflected sunlight and moonlight, but also lasers.

The visible region, 0.4 to 0.7 microns, is largely transparent to the clear atmosphere. During daylight hours, reflectance (albedo) of clouds, sea, forests, solids, etc. can be measured with TV devices or arrays of visible point detectors. The infrared transmission bands of greatest importance are those at 3.3 - 4.2 microns and at 8 - 13 microns (generally narrowed to 10 - 11 microns for better transmission). The 3.7-micron band is ideally suited for detection of sources at temperatures near 1000° K such as volcanoes and forest fires. The 10-micron band is best for detection of sources near 300° K such as the usual earth and ocean surfaces, but the 3.7-micron band can also be used for such measurements. Satellite data in these transmission bands can be used to infer surface temperature. However, in the case of arid, non-vegetated surfaces, emissivities can be much less than one. A notorious example is the 9-micron "reststrahlen" reflectance of quartz, which shows up in desert sands. Corrections must be made for such cases, as well as for atmospheric effects, especially when spectral bands are broad.

The 6.5-micron water vapor absorption band can be used to measure H_2O content. However, evaluation of apparent temperature in terms of true temperature and H_2O content seems difficult. This has been applied mainly in the study of content and distribution of water in the upper troposphere, with the help of simultaneous 8 - 12 micron temperature data.

The 9.6-micron absorption band likewise might be used to measure O_3 content, although UV techniques may be preferable here.

The 15-micron carbon dioxide absorption band has been used to estimate stratospheric emission by CO_2 and thereby an effective temperature of the stratosphere. This gives associated circulation patterns in the stratosphere.

One of the most difficult things to measure in density is cloud height. The 2-micron CO_2 and 0.76-micron oxygen absorption bands have both been suggested as regions to deduce cloud height by the following argument. If a gas has a known mixture in the atmosphere, the optical transmission down to the cloud and back to the satellite depends (aside from a slight temperature term) on the optical path given by the pressure at the cloud top and the angles of incidence and view. The only unknown is the pressure at the cloud top, deduced by the transmission as measured from the relative radiation in the absorbing band and in the nearby continuum. Sometimes stereo techniques can be applied to estimate cloud-top height.

Although little is known of IR spectral emissivity characteristics of ice or snow, the U. S. Army Cold Regions Research and Engineering Laboratory recommends the 10 - 11-micron band for ice inspection instruments. IR definitely presents more information than the visible, especially for ice less than 18 inches in thickness both day and night. Ice can be distinguished from clouds at the same temperature by internal structure and boundary differences. Although surface winds wipe out thermal gradients, they cause microweather patterns which are more apparent from satellite altitude.

Planetary heat balance calculation ideally should be derived from broad band measurements (total IR 8 - 30 microns, total reflected solar radiation 0.2 - 6 microns) but in the past, narrower channels have been utilized (8 - 12 and 0.55 - 0.75 micron bands).

As far as improved sensors are concerned, the consensus of experts is that a better 10-micron detector would be the most valuable addition to the state of the art for weather satellites, as well as satellites with many other missions.

Much of the advanced detector work in this country is aimed at just such an improved device, requiring only passive cooling, but providing much higher sensitivity than thermal devices .

II. SPECIFIC WAVELENGTH BANDS

A. 10 - 12 MICRON REGION

1. Choice of Materials

Although the wavelength region is given here as 10 - 12 μ , the discussions given here are also valid if the region is extended to cover 8 - 14 μ range, if this is considered desirable. This region is of interest because:

- a) atmospheric transmission is at a maximum in this wavelength region.
- b) black body radiator at a temperature around 300^o K has maximum radiant emittance in this region, and
- c) with the advent of the high power CO₂ laser at 10.6 μ , which is proving to be a valuable tool in many solid state studies, it has become increasingly important to have a suitable and efficient detector for the CO₂ laser.

There are detectors whose photoresponses have peak and cutoff wavelengths beyond 14 μ ; Ge:Zn is an example. However these detectors generally have lower D* in the 10 - 12 μ region than most of the detectors to be discussed here. Also, in order to improve the detector performance, it will be necessary to filter out the undesired long wavelength radiation. Hence the discussion is confined to detectors with λ peak in the 10 - 12 μ region and λ_{CO} at 14 - 15 μ . Literature search shows that Ge:Hg is about the only detector that is commercially available for detection at 10 μ . However, the operating temperature is 28^o K and the price is fairly high (around \$3000). Peak value of D* which occurs at 10 μ is given by one manufacturer to be 2×10^{10} (cps)^{1/2}/watt with 2π steradian field of view.

Ge:Zn, Sb is another material that has been used for 10 μ detection in various laboratories. The Semiconductor Products Department of the General Electric Company has developed the technology to grow crystals of Ge doped with Zn and compensated by Sb. However, detectors fabricated from this material have to be cooled to 35^o K for detection at 10 μ and no photoconductivity was observed at 10 μ at 77^o K.

Ge:Be was also investigated as a potential detector for 10 μ region. The first ionization level of Be in Ge is at 0.024 eV which makes it a more suitable detector for around 50 μ ; the second ionization level is believed to be about 0.16 eV which is also unsuitable for 10 μ detection. In addition, the solubility of Be in Ge results in impurity band conduction and low resistivity material which is a disadvantage for charge storage type of readout from arrays made from this material.

Ge:Si alloys doped with proper impurities have also been examined but they do not offer any advantage over Ge doped detectors and add another degree of complexity in achieving the proper alloy composition.

It is known that Mn goes into GaAs as an acceptor with an impurity level 0.1 eV above the valence band. If this state has a reasonably long lifetime and transitions from the valence band to this level have a high probability, it should be possible to use this material as a detector around 10 μ . Although there is no mention in literature of this possibility, the ease with which GaAs: Mn is available makes a laboratory experiment worth the effort.

No quantum counter type of detector has been reported at 10 μ and in fact, it is believed that it is difficult to observe quantum counter action beyond 2 - 3 μ . Nevertheless rare earth ions Sm^{3+} and Eu^{3+} have suitable energy levels to which if optical transitions are probable, quantum counter action may be feasible.

All of the above are extrinsic type of detectors. In the intrinsic category, $\text{Hg}_{1-x}\text{Cd}_x\text{Te}$ and $\text{Pb}_x\text{Sn}_{1-x}\text{Te}$ are the only known materials from which laboratory type detectors have been fabricated. The band gap of these ternary alloys is a function of the mole fraction x of CdTe or PbTe. Although the dependence may not be linear over the entire range of x (from 0 to 1) the curve of E_g vs x is expected to be monotonic and smooth. On the basis, for detection at 10 μ , $x = 0.25$ for $\text{Hg}_{1-x}\text{Cd}_x\text{Te}$ and $x = 0.8$ for $\text{Pb}_x\text{Sn}_{1-x}\text{Te}$. Both of these materials are relatively unknown as compared to Ge. Their crystal growth and purification present problems and their fundamental electrical and optical properties are unknown and not well understood when they are known. Nevertheless, research is continuing in these materials because:

- a) these detectors operate at higher temperature (77° K) than do doped Ge detectors,
- b) they offer possibility of junction formation resulting in electrical isolation and possibly charge storage.
- c) since they are intrinsic detectors, we can expect a higher detectivity ultimately, although at the present state of the art, doped Ge detectors have higher detectivities.
- d) if techniques can be developed to synthesize material with desired value of x , a series of IR detectors can be fabricated to cover the entire range from, say, 2 to 15 μ and beyond.

In view of the fact that doped Ge detectors need to be cooled to cryogenic temperatures and do not lend themselves to p-n junction formation, it is more desirable to concentrate our efforts on $\text{Hg}_{1-x}\text{Cd}_x\text{Te}$ or $\text{Pb}_x\text{Sn}_{1-x}\text{Te}$ which operate at 77° K (although the performance improves as temperature is lowered), offer possibilities of making junction on devices, and are intrinsic photodetectors.

2. $\text{Hg}_{1-x}\text{Cd}_x\text{Te}$

A survey of research done on $\text{Hg}_{1-x}\text{Cd}_x\text{Te}$ shows that crystal growth of a uniform ingot (where x is reasonably constant over the length of the ingot as well as in the transverse plane) is a difficult problem which has not been solved despite several years of research effort.

According to Harman (1) in an ingot with melt composition of $\text{Hg}_{0.8}\text{Cd}_{0.2}\text{Te}$, two adjacent slices (thickness of 2 mm) cut perpendicular to the

growth direction were found by emission spectrographic and polarographic analysis to contain 23 and 57 atomic percent Cd, respectively. Assuming that the material crystallized under essentially equilibrium conditions, the large compositional variations indicate that the liquidus and solidus curves of the pseudo - binary system HgTe - CdTe are widely separated. This is shown in Figure 1 taken from Ref. 1. It is apparent from this partial phase diagram that it is difficult to obtain homogeneous alloys of HgTe - CdTe.

Variations in x mole fraction of CdTe, in compound $Hg_{1-x}Cd_xTe$ result in corresponding variations in the energy band gap of the material. The relationship appears to be linear as shown in Figure 2 (taken from Ref. 1) which summarizes the findings of several workers*. If x varies, say, from 0.23 to 0.57, the energy band gap would vary from about 0.08 eV to 0.7 eV. If we assume that the peak photoresponse of detectors fabricated from these adjacent slices is inversely proportional to their band gap, the peaks would occur at 1.8 μ and 15 μ . Kruse⁽²⁾ shows that detectors fabricated from the same ingot varied in the wavelength of the peak photoresponse from 2 μ to 12 μ

It is apparent from the above discussion that it is difficult to grow uniform and homogenous crystals of $Hg_{1-x}Cd_xTe$ by the Bridgman type of technique; hence detectors fabricated from such crystals would be non-uniform and non-reproducible in their performance. Recently Honeywell has been attempting to grow $Hg_{1-x}Cd_xTe$ epitaxially. However there again problems of non-uniformity and non-homogeneity have been experienced⁽³⁾ and so far no detectors have been fabricated from the epitaxially grown $Hg_{1-x}Cd_xTe$.

The application of zone melting technique in order to achieve a more homogenous ingot is a possibility. However, no such experiment has been reported in literature up to this date. Zone melting, as proposed by Bredt⁽⁴⁾ for the case of SnTe, may also yield material of higher resistivity. Resistivity of $Hg_{1-x}Cd_xTe$ alloys (at 4.2⁰ K) is in the neighborhood of 0.01 Ω cm. It appears that the low resistivity is primarily due to the exceptionally high carrier mobility (as high as 10⁶ cm²/volt-sec in some cases). It is not known what scattering mechanism is dominant and why mobility is so high. In addition to low resistivity, $Hg_{1-x}Cd_xTe$ detectors have the added disadvantage that the change in conductivity, due to incident radiation is only a small fraction of the dark conductivity. It is typical to find dark resistance around 400 Ω and a change of 1 - 2% in resistivity under intense illumination of CO₂ laser at 10.6 μ .

Although nothing has been reported so far, it appears that research is continuing in order to obtain higher resistivity $Hg_{1-x}Cd_xTe$ as well as to make p-n junction devices from this material.

3. $Pb_xSn_{1-x}Te$

Lead salts, PbS, PbSe and PbTe, have been used as IR detectors for several years. However, their cutoff wavelength is below 6 μ . It now appears that by preparing suitable alloys of lead salts, it is possible to decrease the band gap and obtain a material suitable for detection at longer wavelengths.

* The dotted line is for $Pb_xSn_{1-x}Te$ (which will be discussed later) which we have drawn.

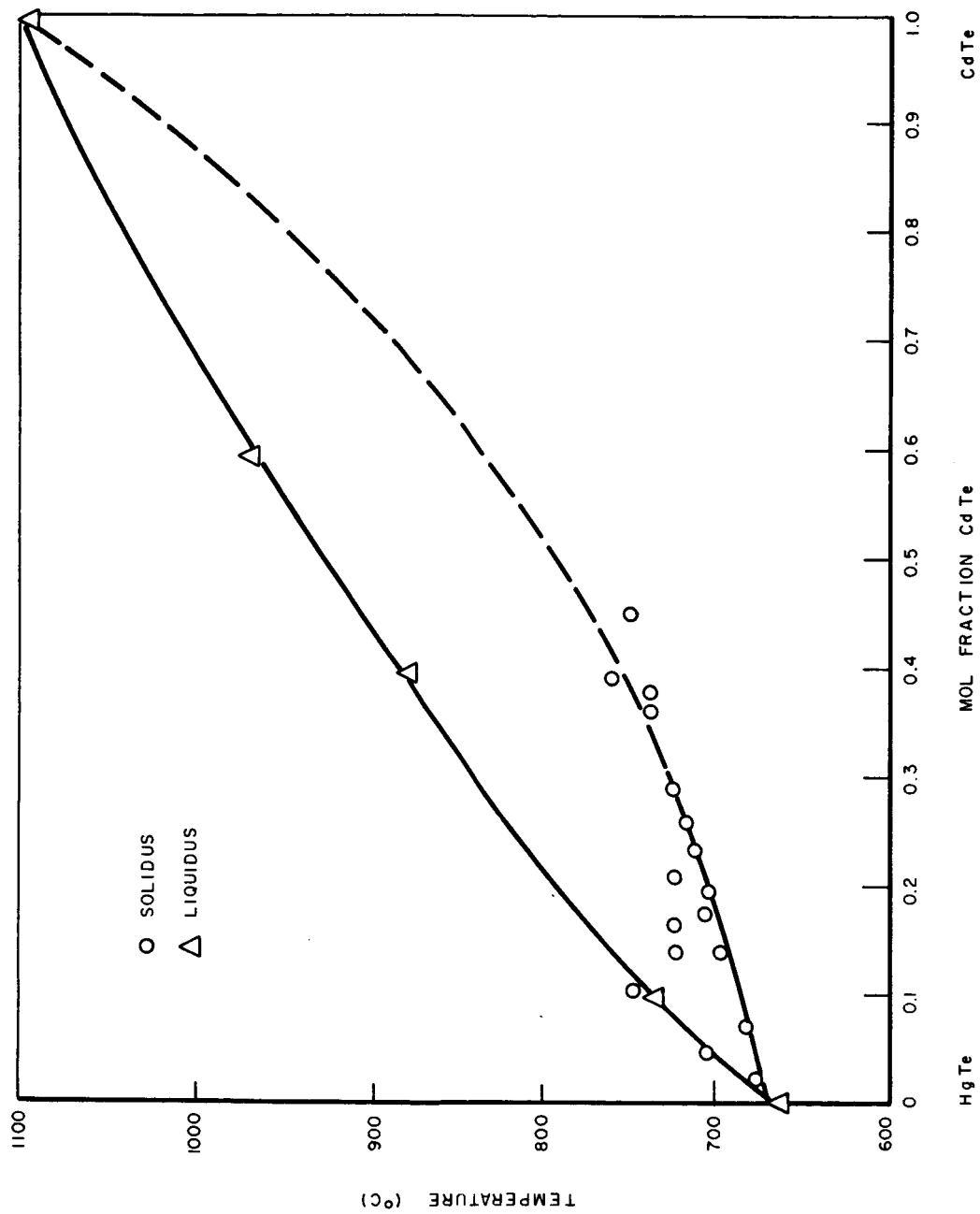


Figure 1. Liquidus - Solidus Curves for HgTe - CdTe

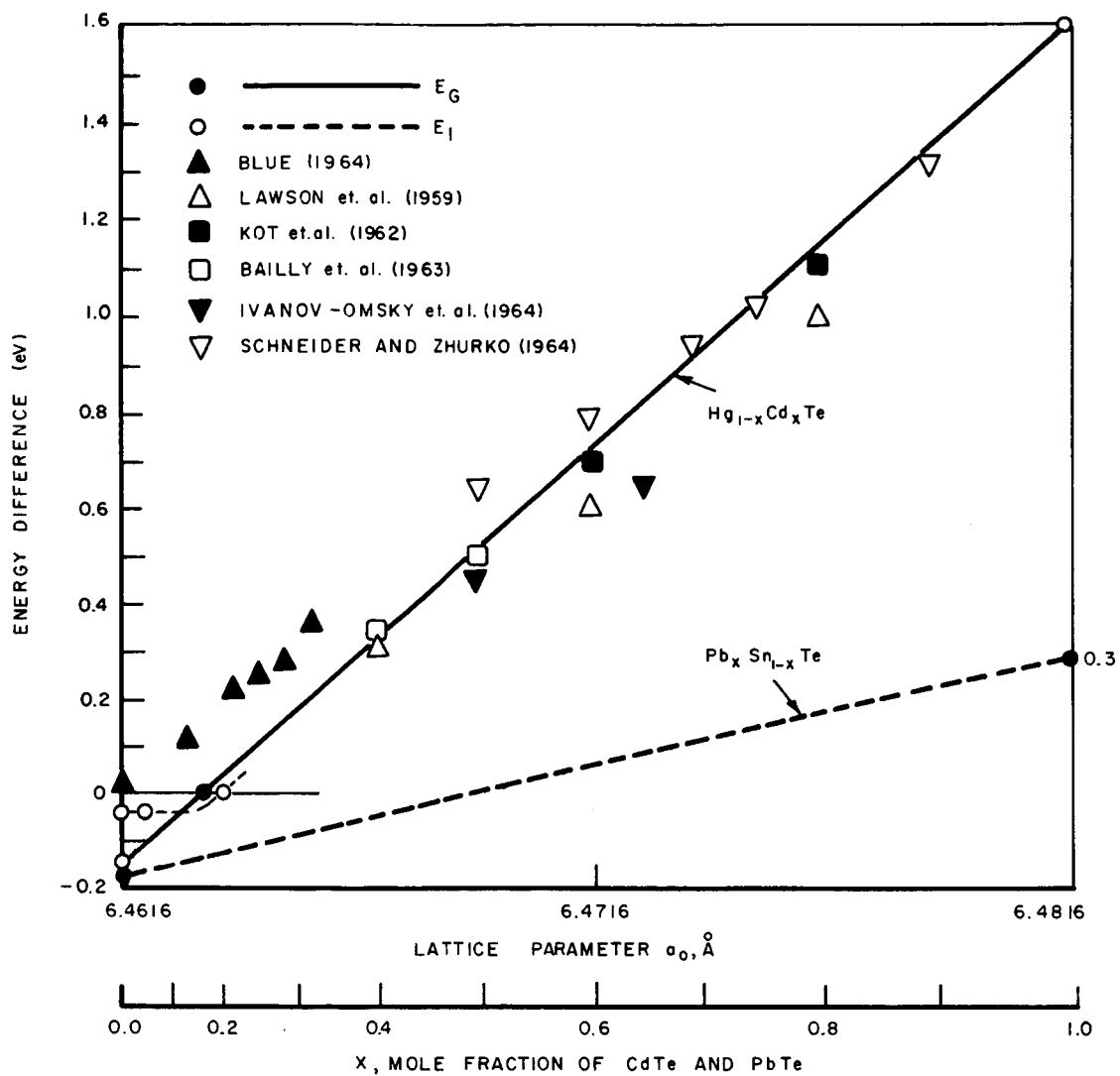


Figure 2. Energy Band Gap Relationship for HgCdTe and PbSnTe

The ternary compound $Pb_x Sn_{1-x} Te$ which is an alloy of PbTe with SnTe, is the latest entry in the field of infrared detector materials, particularly for 8 - 14 μ window detection. So far only photovoltaic mode of operation has been reported.⁽⁵⁾ However, if material with low intrinsic carrier concentration can be synthesized, photoconductive mode of operation should certainly be possible. If the scanty data of Ref. 5 for $Pb_x Sn_{1-x} Te$ and data of Honeywell for $Hg_{1-x} Cd_x Te^*$ are any indication of their performance, it appears that the performance of the two in the 8 - 14 μ region is reasonably similar. From the point of view of synthesizing uniform and homogeneous material, however, $Pb_x Sn_{1-x} Te$ seems to have a decided advantage over $Hg_{1-x} Cd_x Te$ as discussed below.

PbTe and SnTe both have the same lattice structure (NaCl) and although the lattice parameter a_0 is not the same for the two, it is not widely different ($a_0 = 6.454$ for PbTe, $a_0 = 6.313$ for SnTe). It is reasonable to expect that the two are mutually soluble and that the phase diagram would be similar to Figure 1. (The only work on this subject is given in Ref. 6.) If this is the case, it is obvious that if one tries to grow crystal by solidifying from the melt by the normal freezing process, the freezing solid would be inhomogeneous in composition since the liquidus and the solidus curves are widely separated from each other. However for a given variation in x, the mole fraction of PbTe, the variation in energy band gap would be smaller than for the $Hg_{1-x} Cd_x Te$ case, as is obvious from Figure 2 where we have drawn a straight line through the points representing the energy band gap values for SnTe and PbTe. Although no data exist to confirm that this is indeed a straight line, it is reasonable to assume that the energy gap variation with x would be smooth and monotonic. The advantage of $Pb_x Sn_{1-x} Te$ lies in the fact that both PbTe and SnTe are semiconductors of small band gaps and hence compositional variations would cause only small changes in band gap. In contrast, CdTe is a semiconductor of relatively high band gap (1.6 eV) where as Hg Te is a semi-metal of small band gap. Hence alloys of these compounds would show larger band gap variations with composition. Assuming that the synthesis methods are such as to give similar compositional variations, it is apparent that $Pb_x Sn_{1-x} Te$ detectors would not be as widely different in their performance as $Hg_{1-x} Cd_x Te$ detectors. From a practical standpoint, a further advantage results from the fact that one is not working with volatile element like Hg where probability of explosions during material synthesis is high, requiring elaborate laboratory facilities.

Like $Hg_{1-x} Cd_x Te$, $Pb_x Sn_{1-x} Te$ is a relatively unknown material whose basic optical and electrical properties are not known too well and about the synthesis of which there is no reference in literature. It appears⁽⁵⁾ that $Pb_x Sn_{1-x} Te$ is also a low resistivity material with carrier concentration in the range of 2 to $5 \times 10^{17} \text{ cm}^{-3}$ and mobilities in excess of $10^4 \text{ cm}^2/\text{volt-sec}$ at 77° K . The carrier concentration is higher than for $Hg_{1-x} Cd_x Te$ crystals; hence a process like zone melting in order to decrease the carrier concentration would give better results for the case of $Pb_x Sn_{1-x} Te$. Bredt⁽⁴⁾ has proposed this technique although, as with the SnTe proposal, no experimental work has been done to demonstrate the usefulness of the technique. It is encouraging that p-n junctions have been made of $Pb_x Sn_{1-x} Te$ making it a more versatile material for IR detection. Zone melting also has the advantage (true for both $Pb_x Sn_{1-x} Te$ and $Hg_{1-x} Cd_x Te$) that it is possible to control x to a much better degree than one can with the normal freezing method.

* Source of information is classified.

An interesting possibility is to grow $Pb_x Sn_{1-x} Te$ epitaxially if suitable techniques can be developed. One can use a wafer of single crystal PbTe as a substrate on which to grow epitaxial layers of $Pb_x Sn_{1-x} Te$. Proper substrate and source temperatures, suitable chemical reactions and carrier gas would have to be found since nothing appears in print on such a possibility. One must note that while HgTe and CdTe have almost identical lattice constants this is unfortunately not the case for PbTe and SnTe.

4. Experimental Work

For the sake of completeness, we mention the limited experimental work done during this study phase of the contract. This consisted of determining detectivity and responsivity of two $Hg_{1-x} Cd_x Te$ detectors made by Honeywell Corporation. A modulated CO_2 laser and a black body were used as radiation sources for two different experiments. In the former case, a $10.6 \mu CO_2$ laser beam modulated at 120 cps was attenuated and focused on the detector which was cooled with liquid nitrogen and biased at 1 ma. The detector output was amplified, passed through a 1 KC bandwidth filter and read on as RMS reading VTVM. It was found that the amplifier noise was in excess of the detector noise and hence no meaningful value for D^* could be deduced but it is greater than 10^7 . It was also found that the two detectors were considerably different in their dark resistance as well as in their response to apparently identical radiation input.

In order to avoid the problem of noise measurement until a suitable low noise amplifier becomes available, responsivity measurements were made using a black body source at $1000^\circ C$ with 0.2" aperture placed 10 cm away from the cooled detector. Responsivities for the two detectors were different and were calculated to be in the range 5 - 10 volts per watt.

5. Conclusions

Summarized below are the advantages and disadvantages of doped Ge, $Hg_{1-x} Cd_x Te$ and $Pb_x Sn_{1-x} Te$:

Doped Germanium

Advantages:

Fundamental properties and technology better understood.

High resistivity poses less severe problems in scanning.

Arrays may be fabricated using conventional photo-etching techniques.

Material more readily available.

Disadvantages:

Requires cooling to $\sim 30^\circ K$

p-n junctions cannot be made

Extrinsic photoconductor; hence doping and compensation quite critical and absorption coefficient low

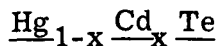
Typical Performance:

$$D_{\lambda}^* = 10^9 - 10^{10} \text{ cm (cps)}^{\frac{1}{2}}/\text{watt}$$

$$\rho = > 10^6 \Omega\text{-cm}$$

$$\tau = \sim 100 \text{ ns}$$

$$R = \sim 10^4 \text{ volts/watt (Ge:Hg)}$$



Advantages:

Intrinsic photoconductor, hence doping less critical and higher absorption coefficient

Operates at 77° K

p-n junctions can be made, hence photovoltaic detection is possible

Peak λ and λ_{CO} can be varied

Disadvantages:

Growth of uniform and homogeneous crystals is a difficult problem

Low resistivity and low $\Delta R/R$ makes scanning difficult

Fundamental properties not well understood

Materials not available

Typical Performance:

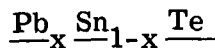
$$D_{\lambda}^* = 5 \times 10^8 \text{ cm (cps)}^{\frac{1}{2}}/\text{watt}$$

$$\mu = 10^5 - 10^6 \text{ cm}^2/\text{volt-sec.}$$

$$\tau = < 20 \text{ ns}$$

$$n = 10^{15} - 10^{16} \text{ cm}^{-3}$$

$$R = 20 - 200 \text{ volts/watt}$$



Advantages:

Intrinsic detector, photovoltaic operation reported and photoconductive operation should be possible

Operates at 77° K

$\Delta E_g/\Delta x$ small

Material preparation easier

Peak λ and λ_{CO} can be varied

Disadvantages:

Low resistivity

Fundamental properties not known

Material not available

Typical Performance:

$$D_{\lambda}^* = \sim 10^9 \text{ cm (cps)}^{\frac{1}{2}}/\text{watt}$$

$$\mu = \sim 10^4 \text{ cm}^2/\text{volt-sec.}$$

$$\tau = \sim 20 \text{ ns}$$

$$n = 5 \times 10^{17} \text{ cm}^{-3}$$

$$R = \sim 50 \text{ volts/watt}$$

We have already indicated the unsuitability of doped Ge as a detector in the 10 - 12 μ region primarily because of the low temperature ($\sim 30^{\circ}$ K) necessary for its performance. It is apparent from the discussion of material synthesis of $\text{Hg}_{1-x}\text{Cd}_x\text{Te}$ and $\text{Pb}_x\text{Sn}_{1-x}\text{Te}$ that $\text{Pb}_x\text{Sn}_{1-x}\text{Te}$ seem a more promising material which is likely to be synthesized with more uniformity and homogeneity resulting in more uniform and reproducible detector performance.

B. THE 2.5 - 5.0 MICRON REGION

1. Choice of Materials

There exists an increasing number of materials to be considered as candidates for use as photon detectors in the 2.5 to 5.0 μ region. A list of most of these materials appears in Table I, along with a summary of their relative D^* detectivities, wavelength of peak response, and response time at typical operating temperatures. The thin film detector materials PbS and PbSe along with the single crystalline InAs and InSb detectors are the more widely used materials for this wavelength range. By way of reference, commercially available PbS photoconductors have the highest detectivity ($D^* \geq 10^{11}$ at temperatures from 77°K to 300°K) while InAs and InSb photoconductors have the lowest detectivities ($D^* \approx 10^8$) at 300°K . The latter materials are much better point detectors when used in the photovoltaic mode - a commercially available InAs photovoltaic detector will typically possess a detectivity of $D^* = 7 \times 10^{10}$ at 196°K .

Additionally, materials such as $\text{InAs}_x\text{Sb}_{1-x}$, $\text{In}_x\text{Ga}_{1-x}\text{As}$, single-crystal Te, and germanium doped with both gold and antimony have been considered. While the first two materials of this group offer much promise for the future in that the peak wavelength for a detector could be chosen by providing the correct value of x for the compound semiconductor, these materials are not generally available, and considerably less is known about their bulk properties than about their major constituent compounds. However, the few experimental detectors made with these materials have appeared promising. Further basic work is needed prior to incorporating these materials into high density arrays. The other remaining compounds require operation at 77°K , which is viewed as being quite restrictive for this program. Photodetectors of the PbS/PbSe and InAs/InSb categories can be operated over a wide temperature range from 77°K up to room temperature. Obviously, a penalty is paid at the higher operating temperature in that the D^* detectivity is lowered by one to two orders of magnitude. Since passive cooling techniques presently limit the minimum allowable operating temperature to around 200°K , the temperatures range from 200°K up to 250°K may be considered as the necessary operating range at the present state of the cooling art. This therefore eliminates the intrinsic germanium and silicon photoconductors as well as tellurium from further consideration under this program.

It would appear, then, that the thin-film photoconductors PbS/PbSe and the single-crystal devices made from InAs/InSb would be the best choice at the present time. The exact choice of one or the other of the two materials in either category is largely dependent on the exact wavelength of interest. InAs and PbS both have cutoff wavelengths well below 5μ . However, their detectivities as well as their operating temperature capabilities offer some advantages over the other compounds; therefore, the ensuing discussion will deal specifically with these two materials rather than just the general categories. A comparison of the advantages and disadvantages of each of the categories is presented in Table II.

TABLE I
 PROPERTIES OF PHOTON DETECTORS FOR
 THE 2.5 TO 5.0 MICRON REGION

<u>Material</u>	<u>Mode</u>	<u>Detectivity</u>	$\frac{\lambda P}{(\mu)}$	$\frac{T}{(^{\circ}K)}$	$t_{resp.}$
InAs	PC	Fair	2.8	195	<20 μ sec
	PV	Excellent	3.3	195	< 1 μ sec
InSb	PC	Fair	5.2	195	<0.2 μ sec
	PV	Good	5.3	77	< 1 μ sec
InAs _x Sb _{1-x}	PV	Good	3.5	200	~1 μ sec
In _x Ga _{1-x} As	PV	Good	2.6	200	-----
Te	PC	Good	3.5	77	80 μ sec
PbS	PC	Excellent	2.5	195	2-5 msec
PbSe	PC	Good	4.5	195	10-150 μ sec
Ge: Au-Sb	PC	Good	3.0	77	<100 μ sec
Ge: Au	PC	Good	5.2	77	<0.1 μ sec
Ge-Si: Au 0.884 - 0.116	PC	Fair	5.5	50	<1 μ sec

TABLE II

COMPARISON OF THIN FILM AND SINGLE CRYSTAL DETECTORS

THIN FILM DETECTORS: PbS, PbSe	
Problems:	<ol style="list-style-type: none">1. Uniformity of D*2. Stability3. Long Time Constant
Advantages:	<ol style="list-style-type: none">1. Highest D*2. Can be Formed on Insulating Substrates3. High Impedance Suitable for Charge Storage Scanning Technique
SINGLE CRYSTAL DETECTORS: InAs, InSb	
Problems:	<ol style="list-style-type: none">1. Uniformity of Material (can be pre-selected)2. Cross-Talk through Substrate3. Relatively Low Reverse Breakdown Voltages as compared with Si and Ge Photodiodes
Advantages:	<ol style="list-style-type: none">1. Can be Formed on Commercially Available Wafers2. Epitaxy Permits Additional Fabrication Techniques3. P-N Junctions quite Suitable for Charge Storage Scanning Technique4. Short Time Constant Compatible with Large Density Array Readout

2. Compatibility with Scan Technique

As discussed in Section III, detectors with high dc resistances allow simpler scanning techniques to be used than do low-resistance devices. Therefore, it is desirable to choose materials that can be used to fabricate detector elements with dark condition dc (as opposed to dynamic) resistances of 10 kilohms or more. With respect to the materials discussed in the previous section, it can be seen that PbS photoconductors satisfy this criteria while InAs photoconductors do not. However, photovoltaic (or reverse-biased photodiode) detectors fabricated from InAs wafers do meet this criterion quite well. Therefore, both of these materials are satisfactory from the impedance standpoint. The only difficulty inherent here is that the reverse breakdown voltage of InAs diodes is limited to a few volts and the scan system must be designed with this restriction.

Another parameter of interest, in high-density detector arrays, is the element response time. In the charge storage mode of interrogation, the element response time must be considerably less than one complete array frame time interval, or the integration properties of this mode of operation are lost. For very long frame times (many milliseconds), either material may be used. However, if the frame time is reduced below several milliseconds, the relatively slower time constant of the PbS photoconductors will result in an overall reduction in system sensitivity.

3. Sensitivity

While PbS photoconductors have the highest D^* detectivity of any detector for this wavelength region, InAs photovoltaic cells operated at 196°K are not greatly inferior. Photovoltaic cells made from InAs are generally more sensitive than photoconductors fabricated from this material. While the impedance levels of the latter limit their usefulness in the charge storage mode, it may be observed that InAs photoconductors are generally epitaxially deposited while the photovoltaic cells are formed via diffusion techniques on single-crystal wafers. The difference in technologies may also explain some of the differences in sensitivity between the two types of InAs detectors.

4. Fabrication Problems

The greatest difference between the state-of-the-art PbS photoconductors and the InAs photovoltaic cells is that the former are formed in situ via thin-film deposition techniques, while the latter are accomplished by standard III-V compound device fabrication processes - masking by SiO_2 deposition (a plasma decomposition process) and photoresist techniques, diffusion, thin-film metal masking and conductor patterns, and etching. This difference is significant because there is less opportunity to control the yield of the in situ prepared devices with respect to both optical and electrical properties. The InAs devices are prepared on grown wafers; while these wafers have variations in their material properties as a function of location across the wafer, many of these properties can be measured directly. Unsatisfactory regions of a wafer or an entire wafer can then be rejected prior to device fabrication. This has already been found to be true with respect to GaAs devices: large variations in resistivity occur across wafers of

semi-insulating GaAs and elimination of low-resistivity sections of the wafer greatly improves device yield and uniformity.

5. Conclusions

From the preceding discussion, it is concluded that yield and degree of uniformity of detector elements are probably more predictable from array to array using the single crystal material. It should also be mentioned that InAs is preferable to thin-film PbS where long term stability is a criterion. Polycrystalline photoconductors are more prone to aging phenomena, although much progress has been made in improving thin film stability in recent years. A list of the properties of the single crystal InAs and InSb detectors is given in Tables III and IV.

C. THE VISIBLE REGION

1. Choice of Detectors

The materials and devices that are used in the visible wavelength are much better understood and consequently under better fabrication control than those in the IR wavelengths. The primary problems in assembling and operating a visible image sensor array are not with the detector element itself, but rather with the array fabrication processing and the system operation of these arrays. Because of this, the visible region provides the best area for study of the system operation problems.

The detectors used in almost all of the recently reported work are either polycrystalline II-VI photoconductors or single crystal silicon. A list of possible materials for the visible along with a tabulation of their particle or quantum gain is given in Table V.

2. Polycrystalline II-VI Photoconductors

The greatest advantage of the II-VI photoconductors can be seen from Table V as the high available gain. Both CdS and CdSe exhibit quantum gains (output electrons/input photons) several orders of magnitude greater than that of other detectors. Their D^* detectivity, although not an absolute comparison for array purposes, is also high; 3.5×10^{14} for CdS, and 2.1×10^{11} for CdSe.

The electrical properties of these materials are also very desirable when used in the charge storage mode of operation (to be discussed in Section III). Surface resistivities of 10^{12} ohms/square and resistivity changes of 5 to 7 orders of magnitude are achievable with these materials.

Fabrication is accomplished by proper doping of the photoconductor powder and subsequent deposition onto a supporting substrate by spraying, screening, evaporation, or sputtering. The latter two provide very thin films and can be used to provide small geometries.

TABLE III

		InAs				PV (Single Crystal)	
		PC (Epi)					
		77°K	195°K	295°K	77°K	195°K	295°K
τ :		400 μ s	<20 μ s	<1 μ s	<1 μ s	<1 μ s	<1 μ s
Noise:		current	current	thermal	current (f < 300) thermal (f > 300)	current (f > 300) thermal (f < 300)	current (f < 100 cps) thermal (f > 100 cps)
Resistance:		100-300 Ω /□	100-300 Ω /□	100-300 Ω /□	40K Ω -2 Meg	3K Ω -7 M Ω	10 Ω - 50 Ω
$D_{\lambda\rho}^*$		2×10^{11} at 3 μ	8×10^9 at 2.8 μ	4×10^7 1.8 - 3.2 μ	from 10^{12} at 2.8 μ	2×10^{11} at 3 μ	5×10^9 at 3.5 μ
Responsivity:					2×10^5 v/w	10^4 v/w	35 v/w

TABLE IV

	InSb			
	PC			PV
	77°K	195°K	295°K	77°K
τ :	$\sim 7.5 \mu s$	$< 0.2 \mu s$	$< 1 \mu s$	$< 1 \mu s$
Noise:	current noise g-r noise above 400 cps	current noise g-r noise	thermal noise limited	current noise, $f < 100$ cps shot noise $f > 100$
Dark Resistance:	2K-25K Ω/\square	25-100 Ω/\square	30 Ω/\square	Dynamic range: 200 Ω - $10^6 \Omega$
Responsivity:	10^4 v/w	150 v/w	2 v/w	$\leq 5 \times 10^5$ v/w
$D_{\lambda\rho}^*$	2×10^{10} at 5.5 μ	5×10^9 at 5 μ	$\sim 10^8$ at 6.5 μ	3×10^{10} at 5.5 μ

TABLE V
DETECTORS FOR VISIBLE WAVELENGTHS

<u>Material</u>	<u>Mode</u>	<u>λ</u>	<u>Quantum Gain</u>
CdS	PC	0.4 - 0.8	$\approx 10^5$
CdSe	PC	0.5 - 1.0	$\approx 10^4$
Si	PC	0.7 - 1.1	≈ 10
Si	Diode	0.4 - 1.1	< 1
Si	Transistor	0.6 - 1.1	$\approx 10^2$
Se	PC	0.3 - 0.5	≈ 1
CdTe	PV	0.4 - 0.84	≈ 1

3. Single Crystal Silicon

Silicon junction devices are photosensitive to light with a peak sensitivity at 0.9 microns. Photodiodes operate with high response throughout the visible region; phototransistors, which provide an amplification of the signal, operate only for the longer wavelengths. For operation at wavelength 0.6 microns, the thickness of the base region required to capture the more energetic photons is not compatible with good transistor action.

Fabrication of arrays of silicon detectors follows the same developments as integrated circuitry. The greatest limitation to high resolution being the isolation required between elements. A great deal of work is currently being undertaken in this area, and any results obtained will be directly applicable to silicon detector arrays. This includes the work in MOS structures where devices have already been placed on 0.002 inch centers.

4. Conclusions

Visible arrays are the closest to operational status of all the wavelengths under consideration. A comparison of the two leading materials is shown in Table VI. There does not appear to be any clear cut advantages of one approach over the other. Thus, without specifying the exact application, parallel development of both techniques appears to be desirable.

TABLE VI

	<u>CdS/Se</u>	<u>SILICON</u>
<u>FABRICATION:</u>	POLYCRYSTAL LARGE AREAS INSULATING SUBSTRATE	SINGLE CRYSTAL LIMITED AREAS CONDUCTING SUBSTRATE
<u>DETECTOR PROPERTIES:</u>	HIGH IMPEDANCE VERY LARGE Δ SIGNAL/DARK SIGNAL	HIGH IMPEDANCE MODERATE Δ SIGNAL/DARK SIGNAL
<u>SCANNING PROPERTIES:</u>	NOT DESIRABLE FOR SCANNER; NEED ADDITIONAL MATE- RIAL FOR CHARGE STORAGE ELEMENTS.	OPTIMUM FOR SCANNER; POSSIBLE TO INCORPORATE CHARGE STORAGE INTO JUNCTION.
<u>STATE OF THE ART:</u>	500-1000 LINES/INCH FABRICATION PROCESSES LIMITED	200-500 LINES/INCH INTER-DEVICE ISOLATION LIMITED

III. ELECTRONIC CIRCUIT TECHNIQUES

1. General Detector Output Characteristics

The basic sampling scheme for an array of detector elements is shown in Figure 3. Ignore for a moment, the integrating elements and consider an array of detector elements connected one at a time to an amplifier which conditions the detector outputs to a useful form " v_o ". Although a mechanical switch is implied in Figure 3, this is only descriptive of the function, which will be accomplished electronically. It is desirable to have a single amplifier and a sampling mechanism for several reasons: 1) a single channel video output is usually required for transmission to a remote point, 2) the amplifier is relatively large in terms of size, weight, and power consumption; hence, an obvious economy in these three factors by sharing among the detector, and 3) cooling requirements at the detector may be contradictory to the operating temperature of the amplifier, hence, it may be located physically remote from the detector array.

For reasonably high level radiation inputs, the simplified system described above is sufficient. However, we are interested in optical inputs approaching the threshold sensitivity of the detector elements, and would like the operation as an isolated detector with its own amplifier. The sampling mode of operation severely restricts the efficiency with which the input photons produce a useful output. This is illustrated in Figure 4. Notice the individual photodetector response, which receives a photon input continuously. If this response is sampled periodically, we will observe the small unintegrated response indicated in the figure and most of the incident photon energy is wasted while other array elements are being sampled. In addition we can expect a practical sampling mechanism to introduce switching noise which could be greater than the detector output.

To solve this problem, an integrating mechanism is introduced at each detector element, as shown in Figure 3. Then we have accumulated the effect of the incident photons at each detector rather than discard them as in the simple scheme. Theoretically, if we sample this integrated response, we will obtain the output amplifier response shown in Figure 4 with the areas under the photodetector response and the output amplifier response being equal. This is a significant increase over the unintegrated response.

To further exploit the threshold of the detector sensitivity in matrix operation, we must consider the general characteristics of detectors operating near this threshold. Figure 5 depicts some of the major considerations. The dark response " V_D " defines the threshold reference and is therefore the center of importance. Two main variations of " V_D " occur as shown in Figure 4. " ΔV_{D1} " is the variation of this parameter due to changes within the detector such as temperature. " V_n " represents a noise component due to amplifier input noise and can be canceled in an integrating system. The actual change of output due to a photon input " ΔV_o " must be interpreted in terms of the above changes and in this sense its lower limit is determined when it can no longer be distinguished from the other parameters of Figure 5.

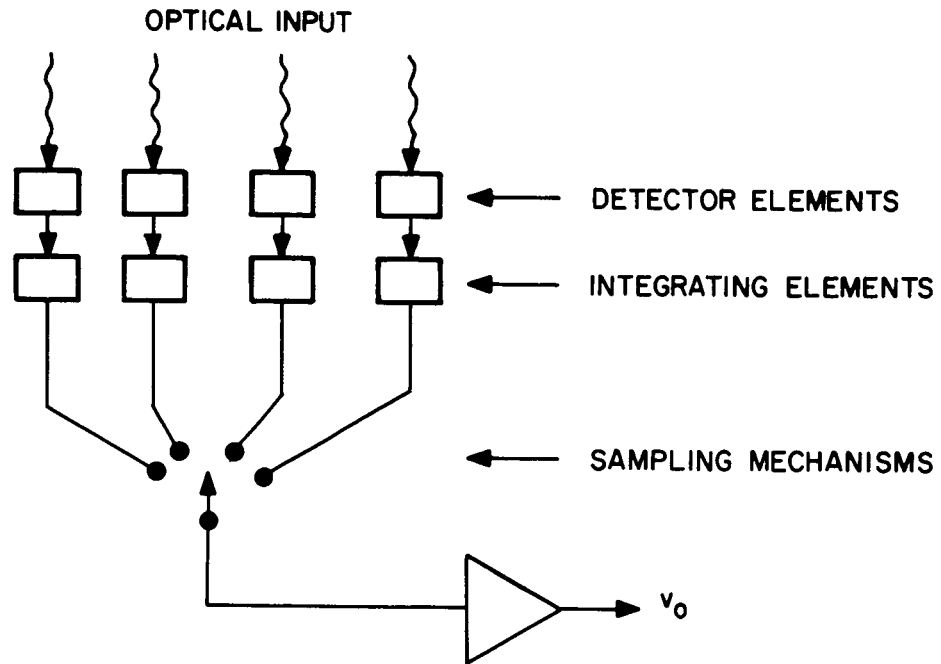


Figure 3. Signal Amplifier and Conditioner

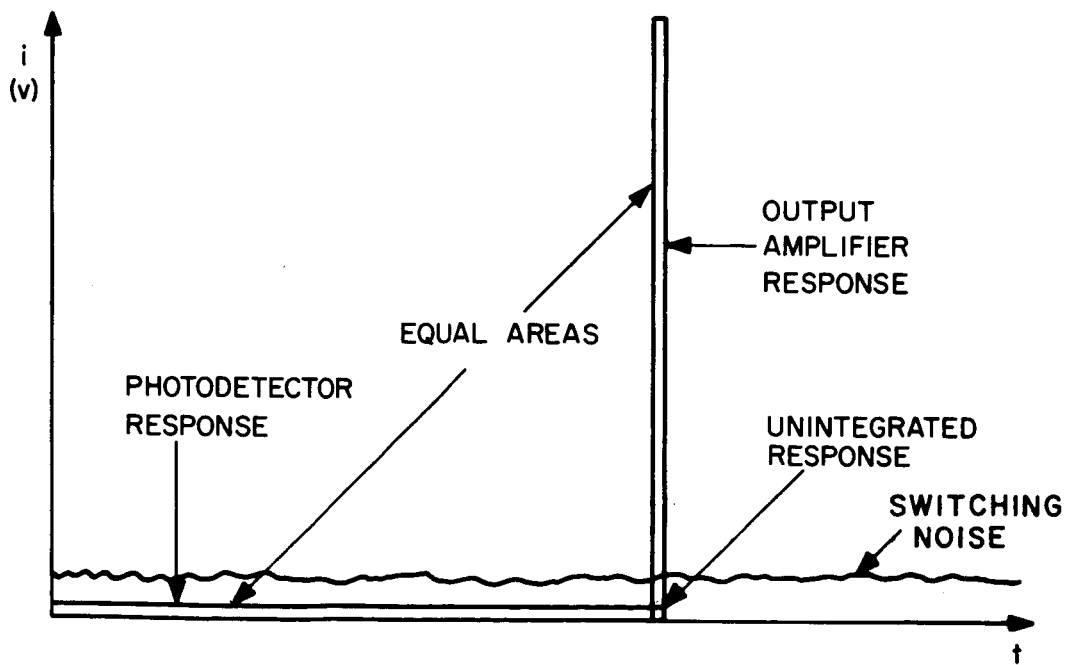


Figure 4. Sampling Mode of Operation

A summary of general detector characteristics is given in Table VII. The parameter $\Delta V_O/V_O$ (referred to Figure 5) adds an extra degree of complexity as previously indicated when it is much less than 10. Then the dark current becomes a very important manufacturing and operating parameter. Also important is the dark impedance of the detector when considering the implementation of the integrating scheme. Several possibilities exist here, some of which are more difficult to implement than others.

2. Charge Storage Operation

The basic charge storage scheme was originally implemented using high impedance detectors as in Figure 6. This implementation utilized the charge stored in a capacitor element to integrate the total number of electrons within flow through the photoconductor. To do this in an economics and realistic fashion, the impedance of the photoconductor must be high so as to allow the use of a small capacitor. Specific values required will depend upon the frame time available to scan the entire array of elements. It is obvious, however, that as the frame time is shortened, the required dark impedance of the detector will be relaxed.

The case of detector elements with very low dark impedance is considered in Figure 7. The circuit shown is the network dual of Figure 6. Implementation of this circuit, however, is not desirable or even possible in high density arrays. For this reason, the equivalent of a high impedance detector is obtained using an active element to transform the impedance level. Such a circuit is shown in Figure 8, where a signal transistor has been shown to provide this function. In addition, the base-collector junctions of the transistor provides a capacitance which can serve as the charge storage capacitor for some combinations of detectors and frame times.

Other active element schemes are possible. Using a small capacitor in a feedback amplifier can provide the equivalent of inductance for an implementation of Figure 7. All of these active element techniques have the disadvantage of placing additional elements into the sensor area, complicating the fabrication of high resolution arrays. Moreover, at low temperature ($< 65^{\circ}\text{C}$) special transistor elements are required.

3. Array Interconnection

The detector elements to be scanned may be assembled in any configuration to suit the optics of the system. This is perhaps one of the more significant advantages of solid state image sensors that is frequently overlooked. Once assembled, however, the individual elements are connected to form an integral electrical matrix, such as in Figures 9 and 10. A one dimensional scan is simply a degenerate case of the matrix and would appear similar to Figure 10 only with single drive lines replacing A B C D and E F G H.

The problem of balancing out the dark current is important to any detector array, and increasingly important at longer wavelengths. Two schemes for accomplishing this are shown in Figures 11 and 12, the first of these using a pair of balanced detectors and the second using a mechanical chopper and a single detector. In either configuration, the operation is based on the use of reversed charge flow through the capacitor during the dark cycle to compensate for leakage currents.

TABLE VII

GENERAL DETECTOR OUTPUT CHARACTERISTICS

	DARK IMPEDANCE	$\frac{\Delta v_o}{V_D}$	WAVELENGTH	TECHNOLOGY
1.	> 10K	> 10	INCREASING ↓ WAVELENGTH ↓	DECREASING ↓ TECHNOLOGY ↓
2.	> 10K	< 10		
3.	< 10K	> 10		
4.	< 10K	< 10		

GENERAL IMPLICATIONS

HIGH DARK IMPEDANCE	⇒	CHARGE STORAGE
LOW DARK IMPEDANCE	⇒	FLUX LINKAGE STORAGE OR EQUIVALENT CIRCUIT
$\frac{\Delta v_o}{V_D} > 10$	⇒	IGNORE DARK CURRENT
$\frac{\Delta v_o}{V_D} < 10$	⇒	DARK CURRENT VERY IMPORTANT OPERATING AND MANUFACTURING PARAMETER

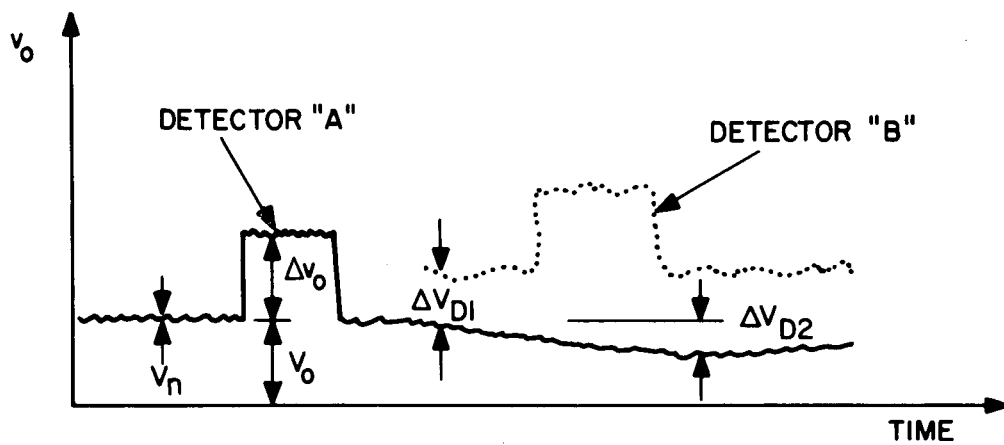


Figure 5. Single Detector Response to Optical Input

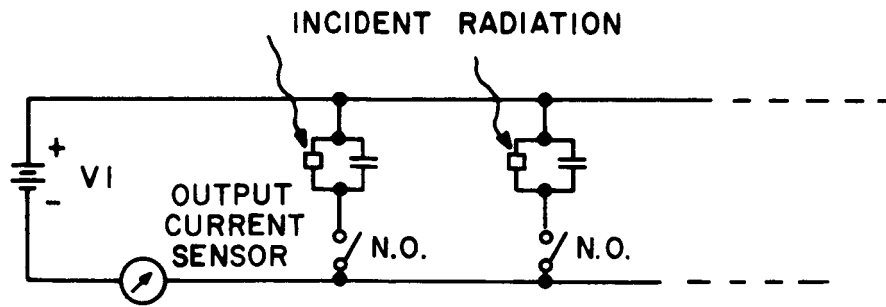


Figure 6. Charge Storage - High Impedance Detectors

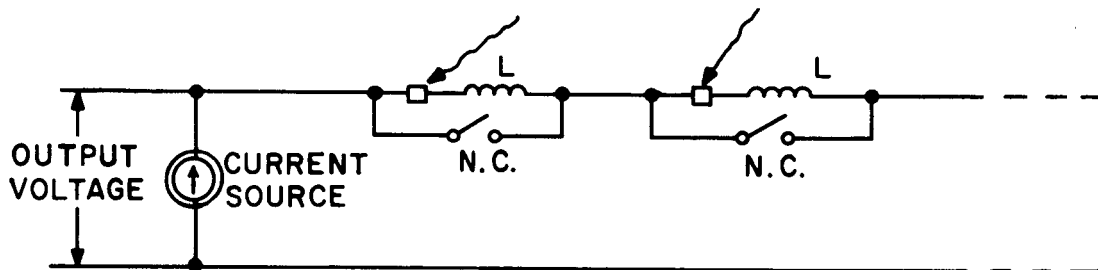


Figure 7. Flux Linkage Storage - Low Impedance Detectors

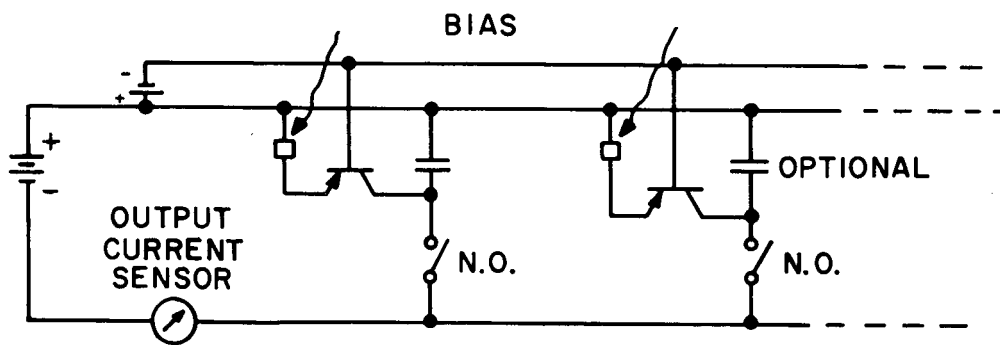


Figure 8. Low Impedance Detectors and Charge Storage

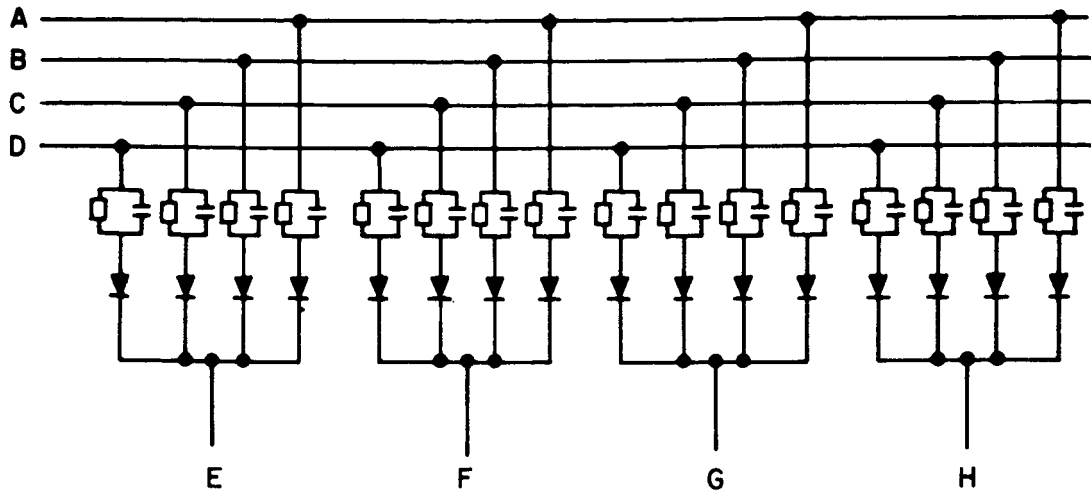


Figure 9. Linear Array Diode Switching

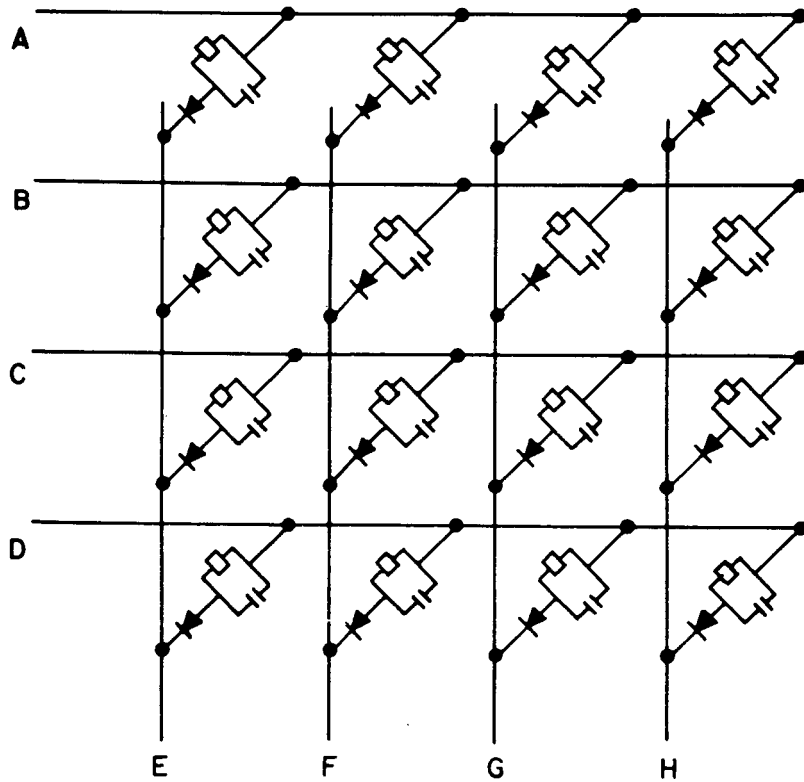
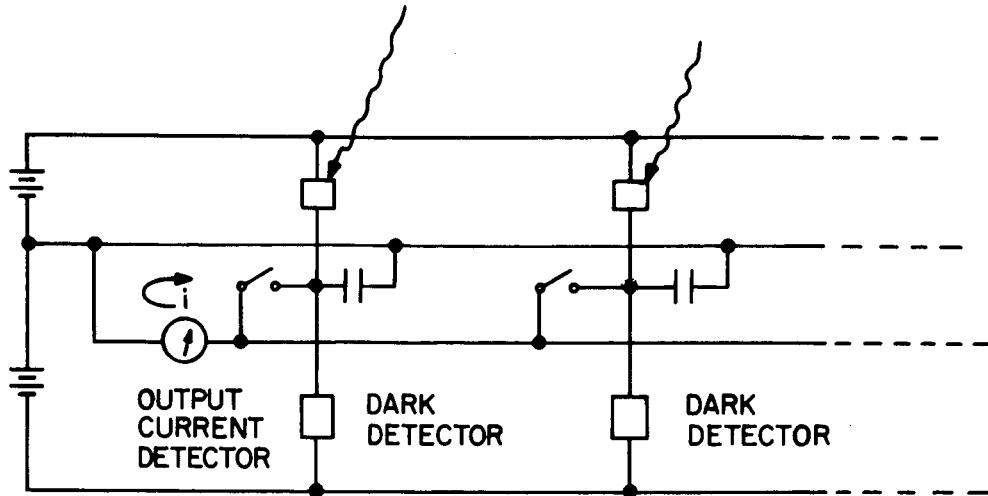
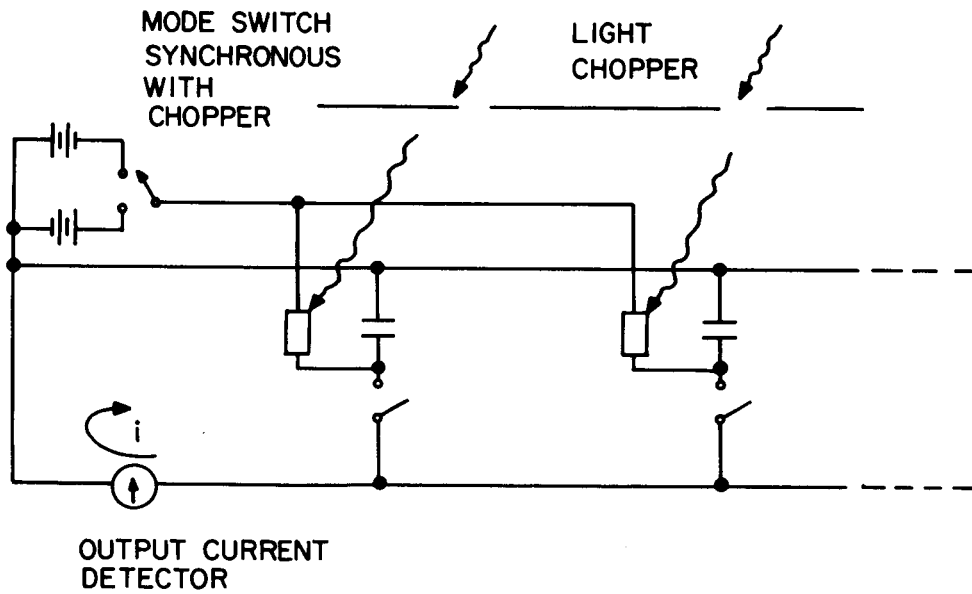


Figure 10. Matrix Array - Diode Switching



MATCHED PAIR DETECTORS FOR BALANCING OUT DARK CURRENT

Figure 11



SYNCHRONOUS LIGHT CHOPPER AND MODE SWITCH FOR BALANCING OUT DARK CURRENT

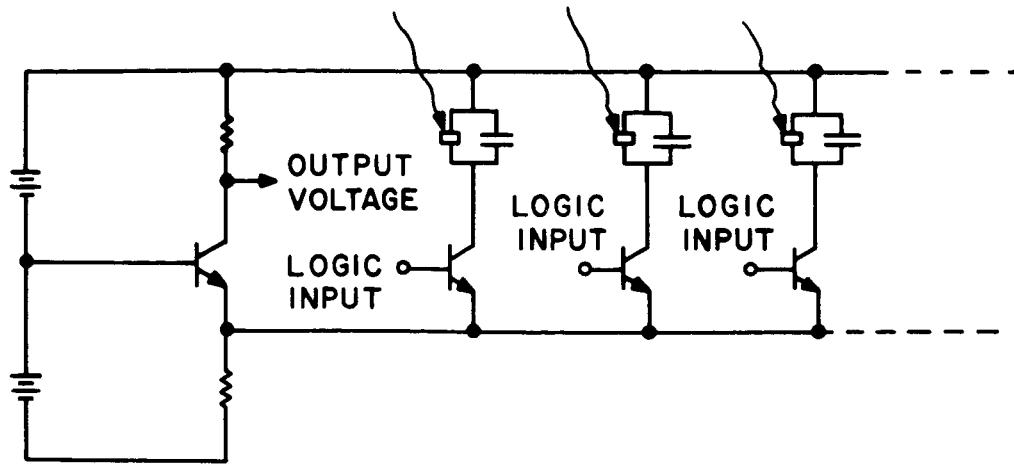
Figure 12

In the figures used up to this point, only schematic switches have been shown. In any implementation however, these switches must take the form of three-terminal switching elements, primarily a transistor. Figure 13 shows a current mode emitter coupled technique to effect the switching of the detector elements. The equivalent of Figure 8 is shown in the implementation of Figure 14. The detectors are shown as being physically remote from the transistor switching elements because of the temperature limits.

4. Conclusions

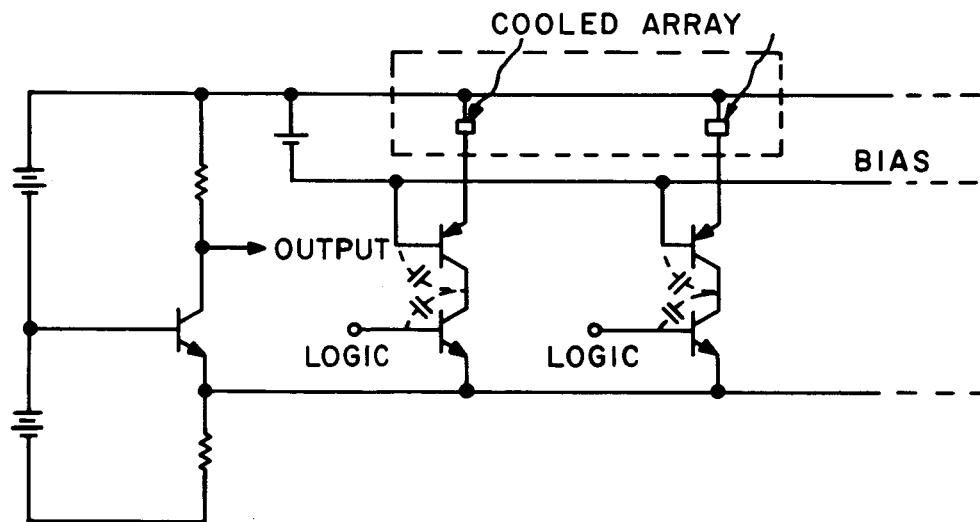
Specific implementation of the scanning system is shown to be a function of the detector impedance, switching ratio, frame time, and required cooling conditions. Nevertheless, the following general conclusions can be stated for the scanning:

1. Large array will require integrating scheme for efficiency.
2. Low impedance detectors will be converted to high impedance.
3. Dark current considerations may be appreciable portion of operating and manufacturing consideration.
4. Dark current can be subtracted at matrix element using several techniques.
5. Switching functions are efficiently performed by solid state components, particularly diodes, bipolar transistors or FET's.
6. Final useful hardware will contain a combination of several of these ideas.



**CURRENT-MODE EMITTER COUPLED DRIVERS
HIGH IMPEDANCE DEVICES**

Figure 13



**LOW IMPEDANCE CIRCUIT USING B-C
CAPACITY OF TRANSISTOR FOR STORAGE**

Figure 14

IV. CONCLUSIONS AND RECOMMENDATIONS

A. CONSIDERATIONS

The conclusions and recommendations which are presented here are aimed at the fulfillment of the second phase of the present contract. For this reason, the estimated goals have a time and level of effort restraint. However, in order to make the conclusions of a more general purpose, longer range goals are also presented. As in the preceding sections of this report, the discussion is divided according to the three wavelength bands.

The visible region can be characterized by its advanced stage of device development, a high level of effort placed in array fabrication as a result of similarity to integrated circuit techniques, and a rather broad interest in applications. Several programs have been undertaken in this wavelength, although all are in the laboratory stage of development. The interest in the application is obviously high, since much of the information which is used in imaging systems lies in the visible. Interest is also spurred by the obvious commercial value of a solid state image detector to the television industry.

The 2.5 to 5 micron region does not have the advantage of the device array fabrication techniques of the visible, although detector elements have been built and operated in small arrays. Some materials, particularly InAs and InSb can be grown with moderate uniformity. The amount of effort directed at producing a imaging system for this wavelength is quite small, however, and much effort can be expected before usable systems are available. The applications to meteorology were described in Section I. B., and these appear to be some of the prime motivations for the use of this wavelength. Another important consideration is the ability to use scanning techniques quite similar to those developed or under development for the visible region. The one significant difference between the 2.5 - 5 micron region and the visible is the need for cooling. While not as severe as that required for 10 - 12 microns, the lower temperature operation provides a definite limit on the choice of devices used in the scanning.

The 10 - 12 micron region is the least developed of all the regions from the point of view of materials, detectors, sensitivity, and scanning. The greatest reason for pursuing this wavelength is the long list of application for 10 - 12 micron wavelengths. Whereas the other wavelengths require device or array work, basic material work is required for 10 - 12 microns. Cooling is also a rather severe limitation in that only active cooling apparatus will provide the 77° K or lower temperatures required. The high interest in the meteorological applications, plus the new uses of 10.6 micron laser radiation detectors have intensified the material and device work necessary to implement image sensors at this wavelength.

A comparison of these considerations is shown in the graph of Figure 15

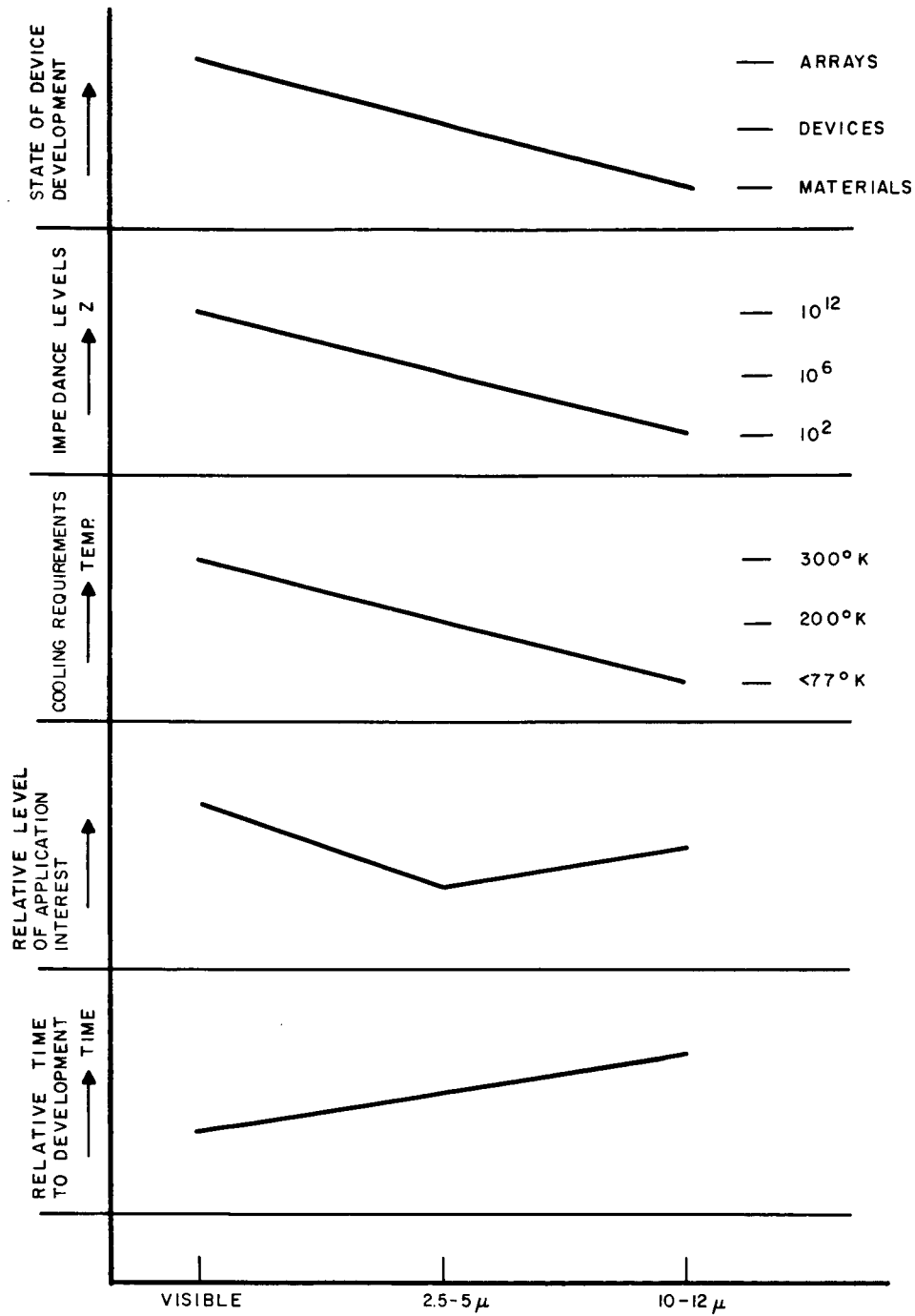


Figure 15. Comparison of the Three Wavelengths of Interest

B. RECOMMENDATIONS

Based on the study undertaken during Phase I of this program the following recommendations are made for the remainder of the program.

Visible: No work should be done in this wavelength because of the existing level of effort maintained by other contracts in NASA and elsewhere. In addition, the continuing development of new isolation techniques in the integrated circuits industry will be directly applicable to detector arrays as they are refined.

2.5 - 5 Microns: A complete scanning system should be built for this wavelength. The availability of materials as well as the general III-V compound processing technology insure a reasonable probability of fabricating usable arrays. Moreover, this wavelength region will provide information on the use of cooling techniques on the array and scanning approaches developed under visible programs.

10 - 12 Microns: A materials effort program aimed at devices and arrays compatible with electronic scanning should be maintained. The many applications utilizing this wavelength indicate that these devices will eventually be required.

V. REFERENCES

1. T. C. Harman, "Properties of Mercury Chalcogenides", this will be published as a chapter in a book on II-VI Compounds, edited by M. Aven and J. S. Prener.
2. P. W. Kruse, "Photon Effects in $\text{Hg}_{1-x}\text{Cd}_x\text{Te}$ ", Applied Optics, June 1966.
3. Honeywell Corporation, Quarterly Progress Reports, Contract AF33(615)-2322, 1 October 1965 to present, "Intrinsic Infrared Detector Development".
4. General Electric Company, Technical Proposal, "PbTe-SnTe Alloys with Small Band Gap" prepared for U. S. Army Research and Development Laboratories, Fort Belvoir, Va., 12 October 1966.
5. I. Melngailis and A. R. Calawa, "Photovoltaic Effect in $\text{Pb}_x\text{Sn}_{1-x}\text{Te}$ Diodes", Applied Physics Letters 9, No. 8, 15 October 1966.
6. Abrikosov, N. Kh., Dvuldina, K. A., Danilyan, T. A., Journal of Inorganic Chemistry (USSR), Vol. III, 1958, pp. 1632-1636.